

**Development of Monolithic Active  
Pixel Sensors  
in a 0.13  $\mu\text{m}$  Triple Well  
CMOS Technology with  
In-Pixel Full Analog Signal Processor**

F.Forti

On behalf of the SLIM5 Collaboration

# Outline

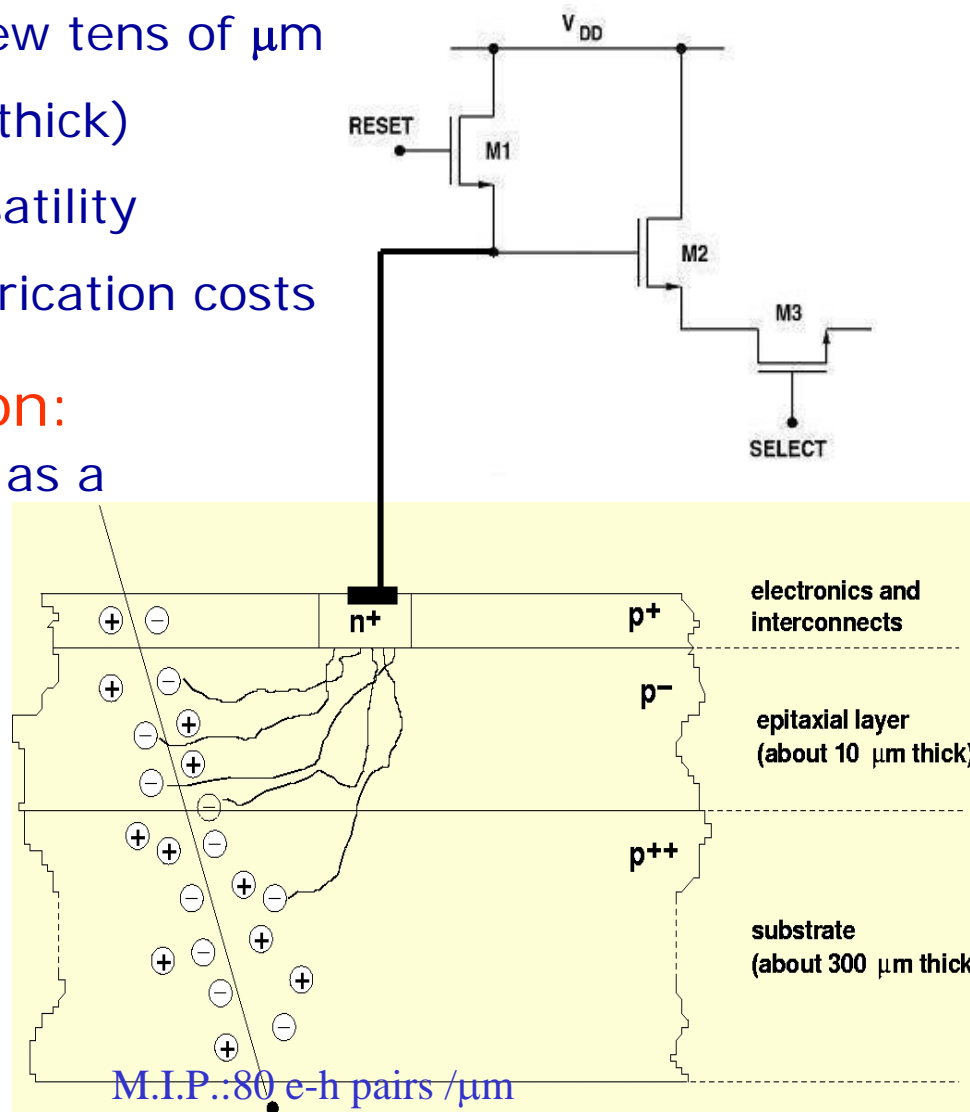
- Introduction: standard MAPS for vertex detectors in HEP
- The new features of our MAPS:
  - deep n-well collecting electrode
  - signal processing at pixel level
- The characterization of the 1<sup>st</sup> prototype “Apsel0”:
  - Front-End Electronics
  - Sensor response to:
    - soft X-rays from  $^{55}\text{Fe}$
    - $\beta$ -rays from  $^{90}\text{Sr}/^{90}\text{Y}$
- 2<sup>nd</sup> prototype “Apsel1”:
  - FEE improvements
  - Single channel response to ionizing radiation
  - Test on the matrix
- Next submission: “Apsel2”
- Conclusions

# Conventional CMOS MAPS

- Several reasons make them very appealing as tracking devices :
  - detector & readout on the same substrate
  - wafer can be thinned down to few tens of  $\mu\text{m}$
  - radiation hardness (oxide  $\sim$  nm thick)
  - high functional density and versatility
  - low power consumption and fabrication costs

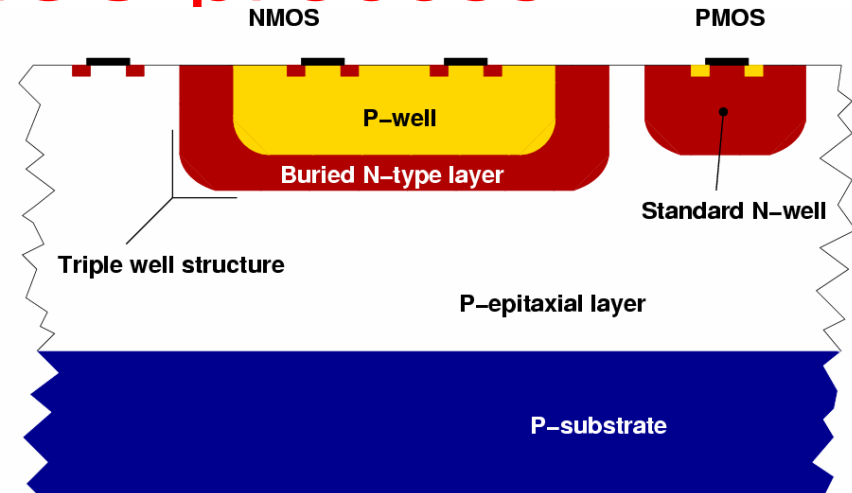
## Principle of standard operation:

- The undepleted epitaxial layer acts as a potential well for electrons moving by diffusion
- Signal ( $\sim 1000 e^-$ ) collected by the n-well/p-epi diode
- Charge-to-voltage conversion provided by the sensor capacitance
  - small collecting electrode
- Extremely simple in-pixel readout (3T NMOS, PMOS not allowed)
  - sequential readout



# Triple well CMOS process

- In triple-well CMOS processes a deep n-well is used as a shielding frame against disturbances from the substrate to provide N-channel MOSFETs with better insulation from digital noise



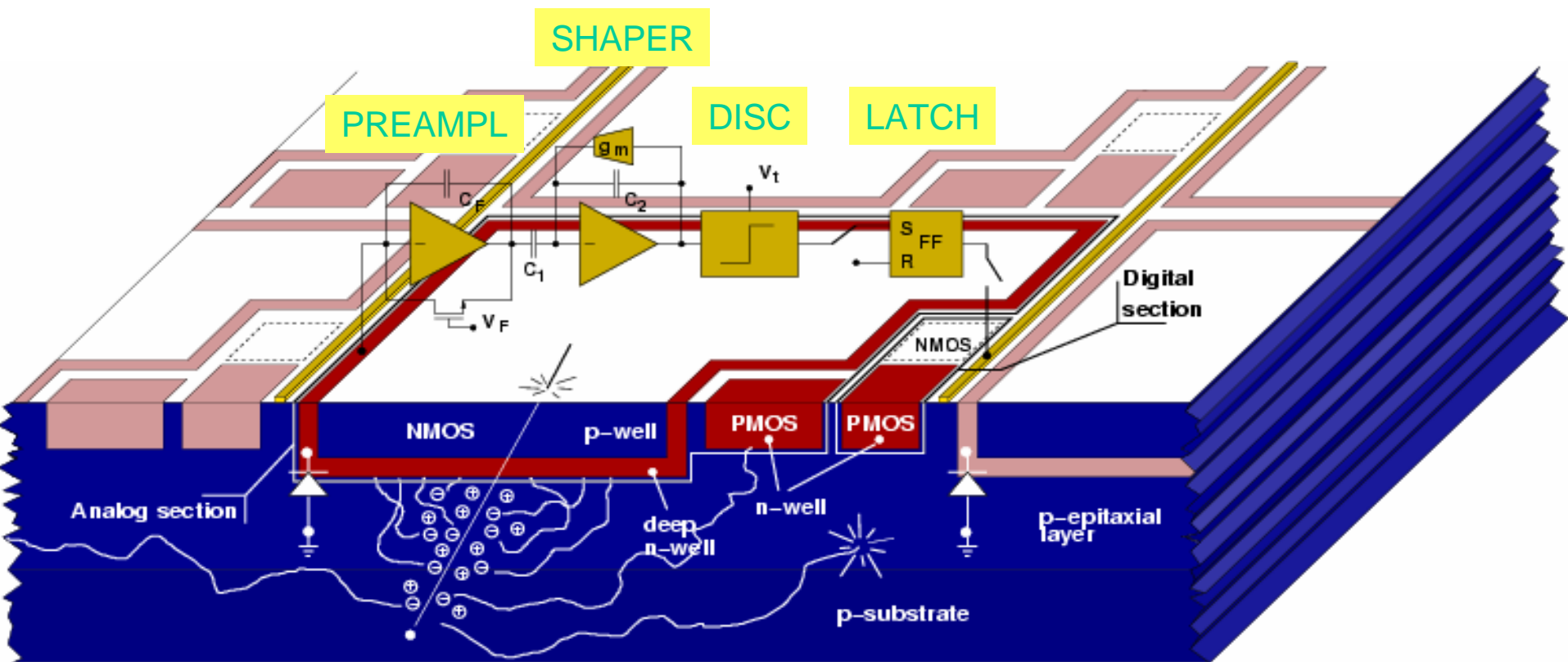
## The new design features of our CMOS pixels:

- The **deep n-well** can be used **as the collecting electrode**\*
- NMOSFETs can be integrated both in the epitaxial layer or in the nested p-well. p-channel MOSFETs are integrated in standard n-wells
- A **full signal processing** circuit can be implemented **at the pixel level** overlaying the NMOS transistors on the collecting electrode

\* Use of the deep n-well was proposed by Turchetta et al. (2004 IEEE NSS Conference Record, N28-1) to address radiation hardness issues

# Deep n-well sensor concept (I)

Standard signal processing chain for capacitive detector (i.e. hybrid-pixel-like) implemented at pixel level:



- Charge-to-Voltage conversion done by the charge preamplifier
- The collecting electrode can be extended to obtain higher single pixel collected charge (the gain does NOT depend on the sensor capacitance)

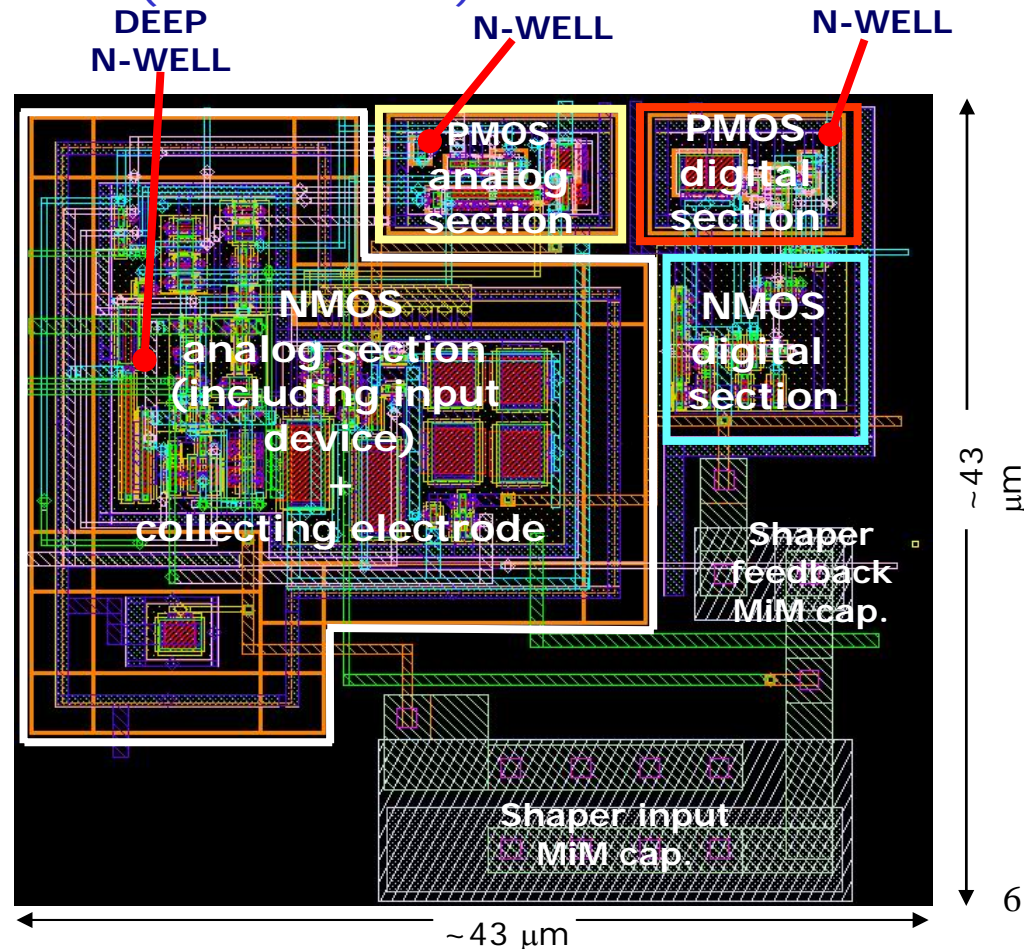
# Deep n-well sensor concept (II)

- NMOS devices of the analog section built over the deep n-well
- Included complementary devices needed for CMOS design
- Fill factor  $\equiv \text{Area}(\text{deep n-well}) / \text{Area}(\text{total n-wells})$

( $\geq 0.85$  in the prototype test structures)

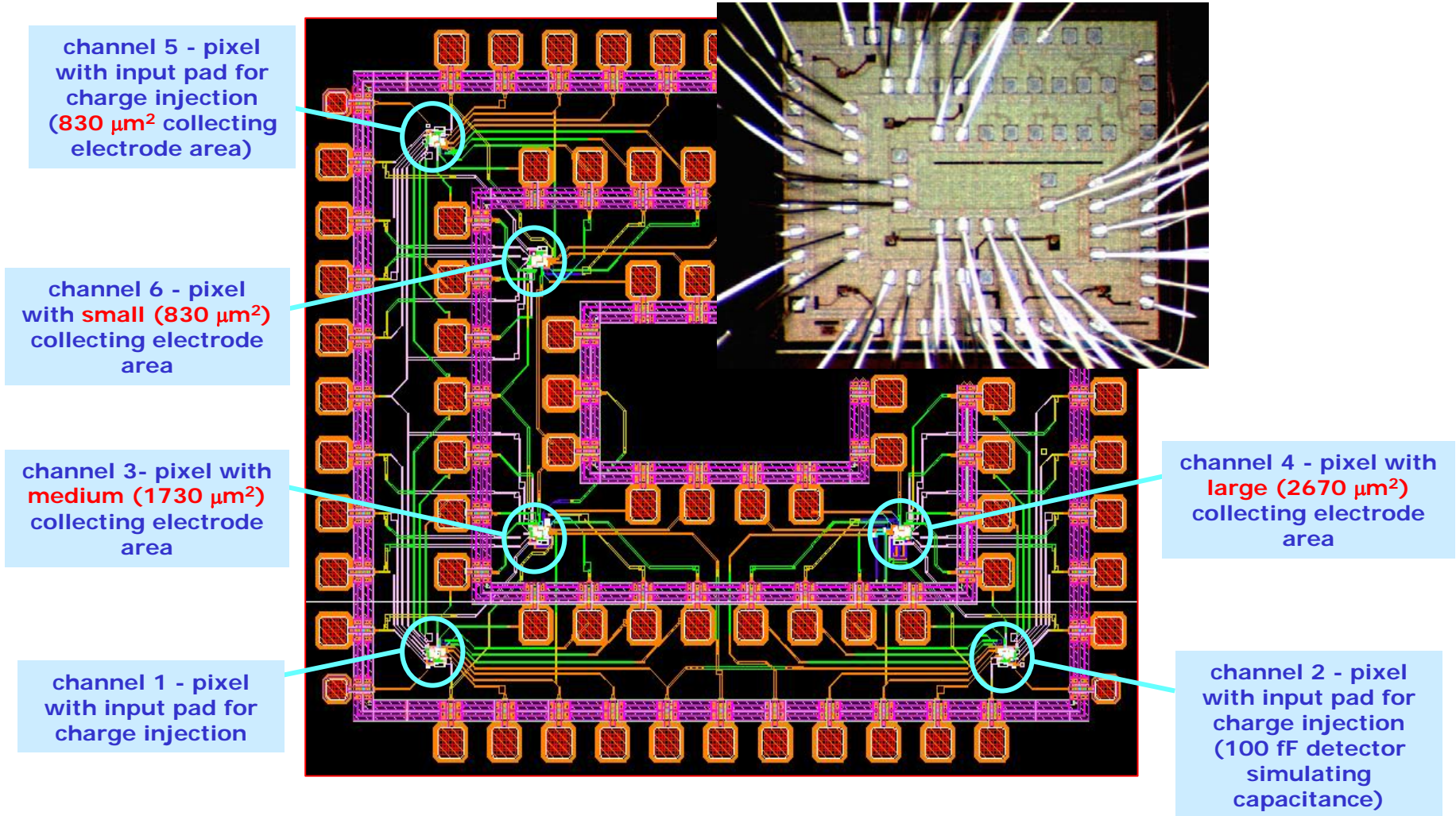
- The readout scheme well fits into already existent architectures for data sparsification at the pixel level to **improve readout speed**

Pixel cell layout



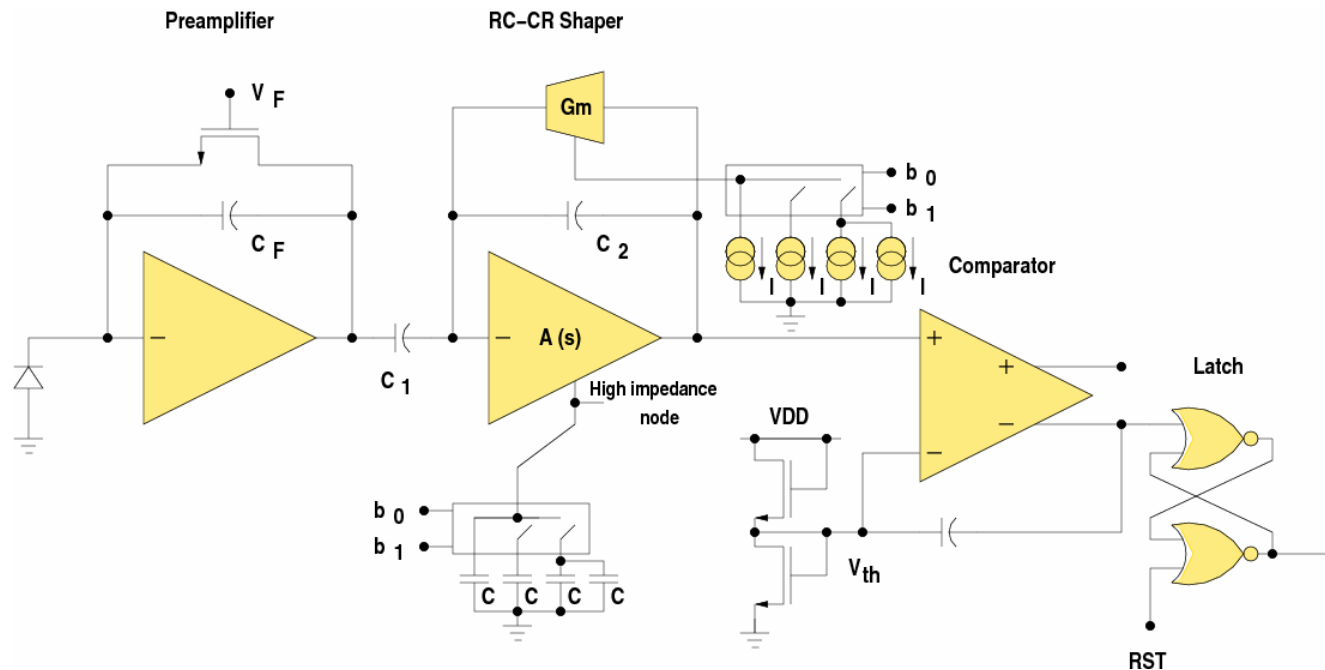
# 1<sup>st</sup> Test Chip Layout: apsel0

0.13  $\mu\text{m}$  CMOS HCMOS9GP by STMicroelectronics: epitaxial, triple well process (available through CMP, Circuits Multi-Projets)



Ch. 1-2-5 have integrated injection capacitance for readout electronics characterization

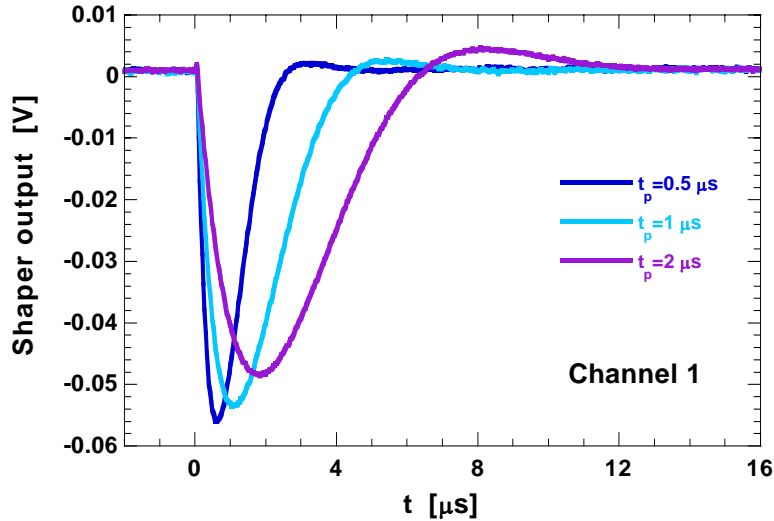
# Pixel level charge processor



- High sensitivity charge preamplifier with continuous charge reset (n-well/p-epi diode leakage current)
- The preamplifier input provides the bias to the deep n-well (0.3 V)
- Input device ( $W/L=3/0.35$ ) optimized for a 100 fF detector capacitance and operated at a drain current of about  $1 \mu A$

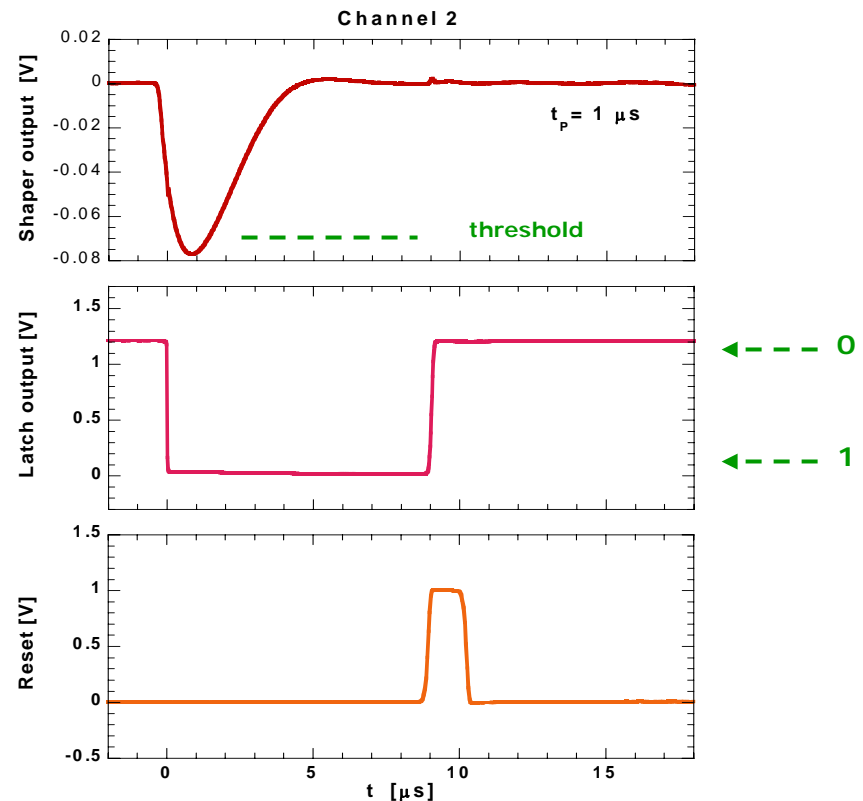
- RC-CR shaper with programmable peaking time: 0.5, 1 and  $2 \mu s$ . Conservatively chosen to avoid ballistic deficit
- A threshold discriminator is used to drive a NOR latch featuring an external reset
- Power consumption:  $10 \mu W$

# Front-End Electronics Characterization



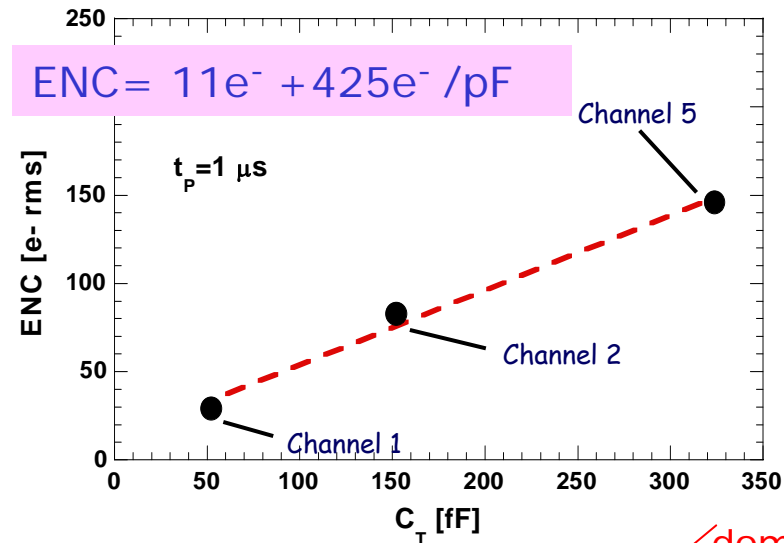
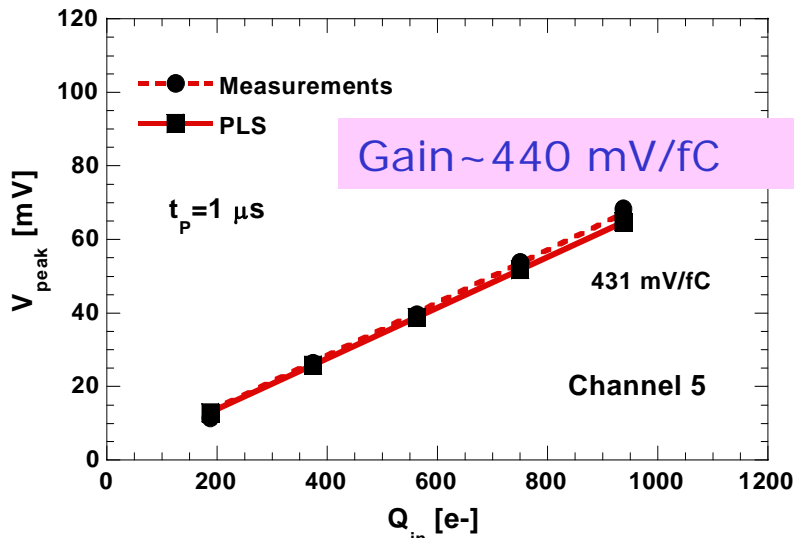
- Shaper response to a 560 e<sup>-</sup> input charge at the three different peaking times
- About 15% variation in peak amplitude moving from the shortest to the longest peaking time

- Slight overshoot probably due to residual parasitic coupling between preamplifier input and shaper output
- The latch preserves the signal until it has been retrieved
- External reset signal sent to the latch returns it to the initial condition



# Gain & Noise Measurements

- Charge sensitivity and Equivalent Noise Charge measured in the three channels with integrated injection capacitance  $C_{inj}$
- Good agreement ( $\sim 10\%$ ) with the post layout simulation results (PLS)



- Equivalent Noise Charge is linear with  $C_{Tot}$

$$C_{Tot} = C_D + C_F + C_{inj} + C_{in}$$

$C_D$  = detector capacitance ( $\sim 270$ fF ch.5,  $C_D^{MIM} = 100$ fF)

$C_F$  = preamplifier feedback capacitance (8 fF)

$C_{inj}$  = test inj. Capacitance (30 fF)

$C_{in}$  = preamplifier input capacitance (14 fF)

$$ENC = C_T \sqrt{S_W \frac{A_1}{t_p} + A_2 A_f}$$

dominant contribution

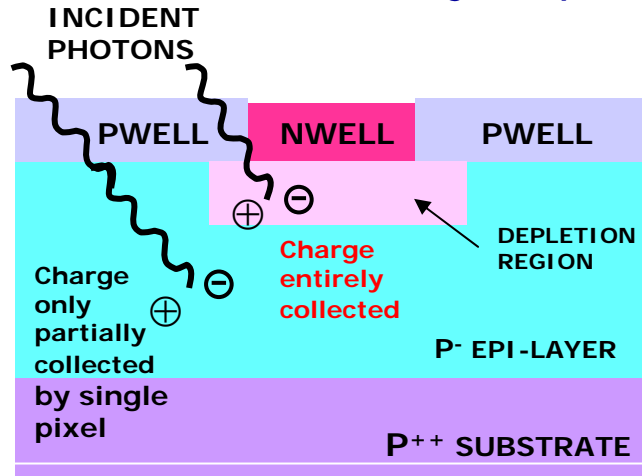
$S_W$  = series white noise spectral density

$A_f = 1/f$  noise power coeff.,  $A_1, A_2$  = shaping coeff.

- Sensor capacitance higher than initially expected: noise performance greatly affected. Room for improvement in next chip submission

# Calibration with soft X-rays from $^{55}\text{Fe}$

X-ray from a  $^{55}\text{Fe}$  source used to calibrate pixel noise and gain in channels with no inj. capacitance



5.9 keV line  $\approx$  1640 e/h pairs:

- charge entirely collected

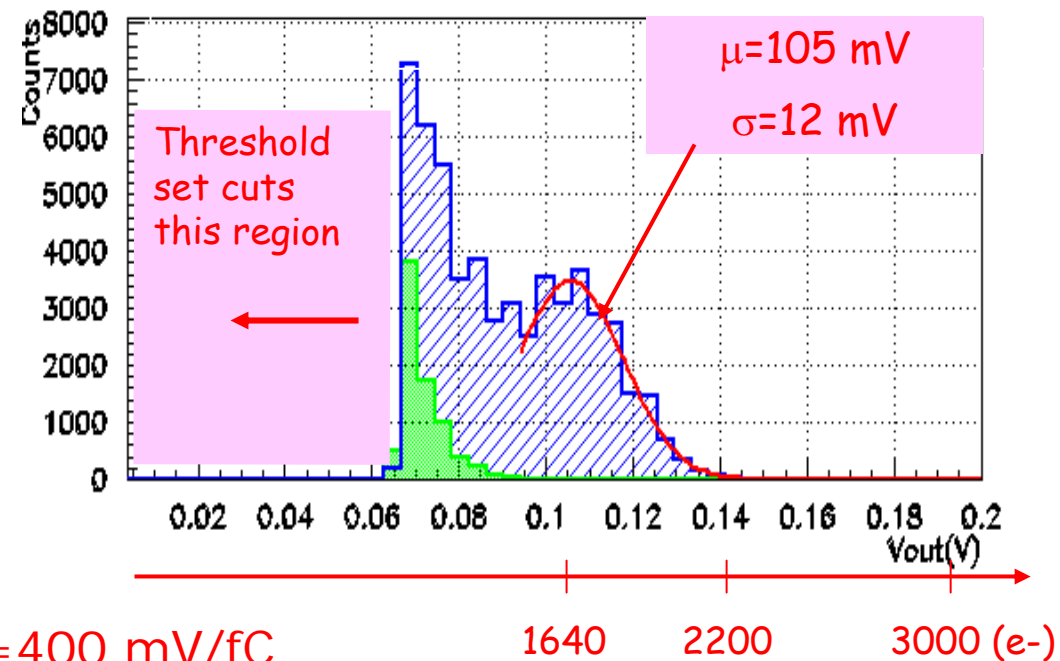
→ clear peak @ 105 mV → gain=400 mV/fC

- charge only partially collected → below 100 mV excess of events w.r.t. noise only spectrum

- Calibration with  $^{55}\text{Fe}$  source in fair agreement with results obtained both with external pulser tests and with PLS (ENC=140 e-, gain=430 mV/fC expected, 125 e- and 400 mV/fC measured)

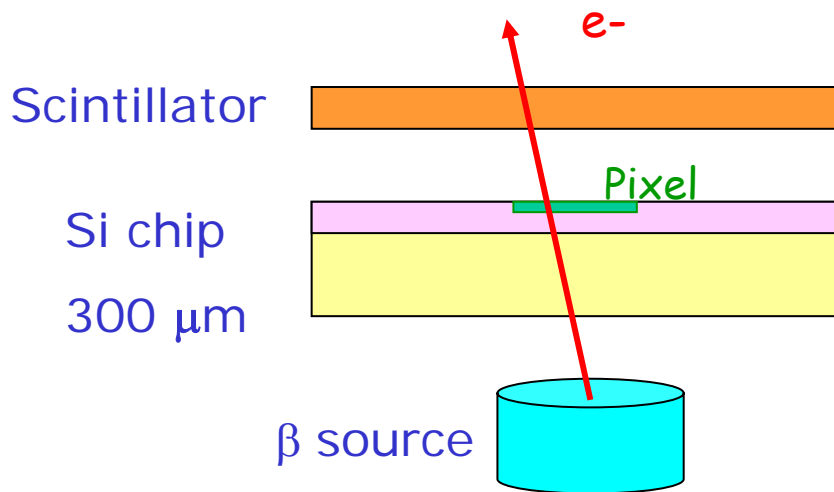
Peak value of the shaper output:

- blue -  $^{55}\text{Fe}$  source (5.9 keV)
- green - no source



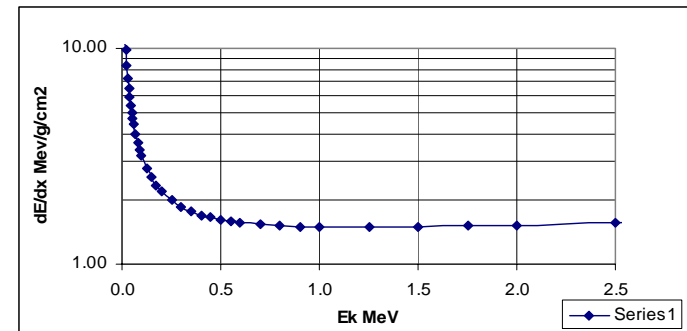
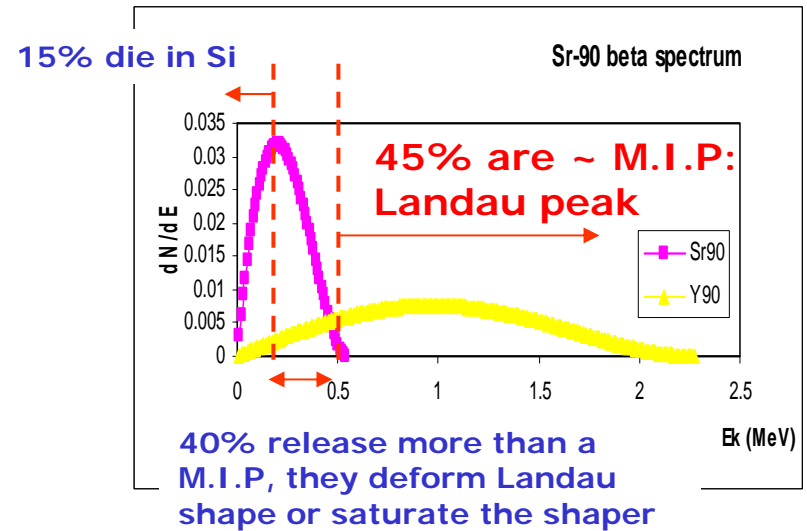
# Response to $\beta$ -ray from a $^{90}\text{Sr}/^{90}\text{Y}$ source

Response to M.I.P from the beta source used to measure S/N ratio



Acquisition triggered by the coincidence (scintillator AND pixel) signal above threshold, set @  $\sim 0.5$  MIP

Electrons from  $^{90}\text{Sr}$  and  $^{90}\text{Y}$

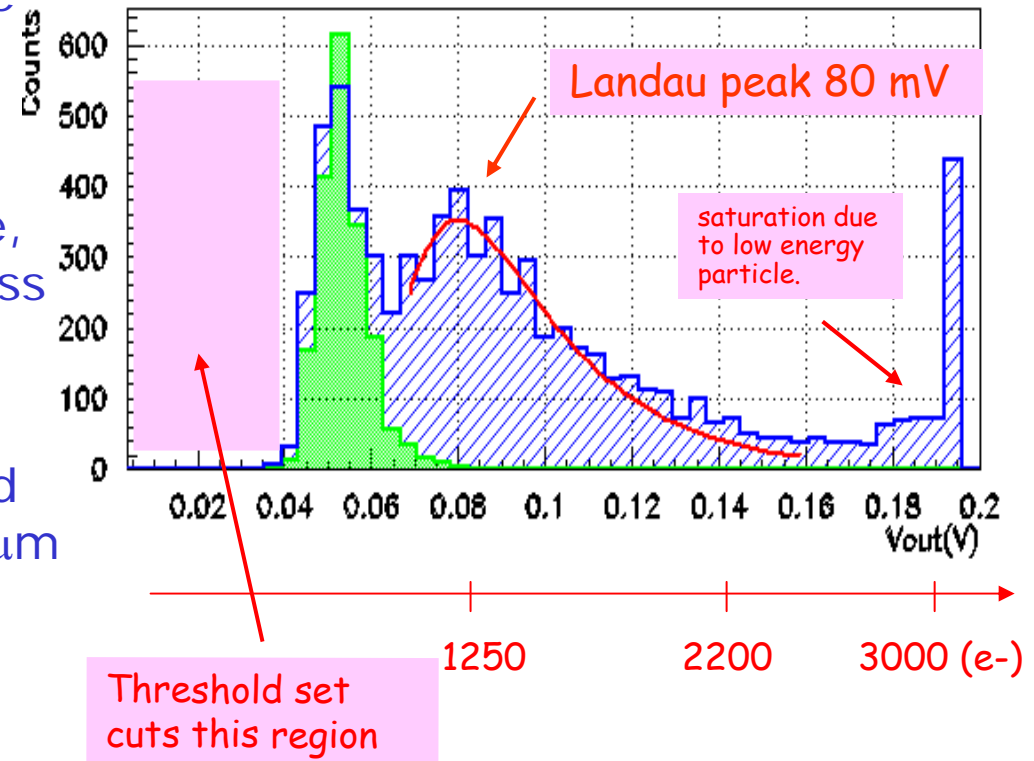


# Results from $\beta$ -ray

- The spectrum clearly shows a Landau peak @80 mV
- Using M.I.P signal and average pixel noise:  
 $S/N=10$
- Using gain measured with  $^{55}\text{Fe}$ , M.I.P most probable energy loss corresponds to about 1250 e-
- Fair agreement with sensor simulation:  $\sim 1500$  e- expected for p-epi layer thickness  $> 15 \mu\text{m}$
- Some hint on the process secrets: p-epi layer is thick!

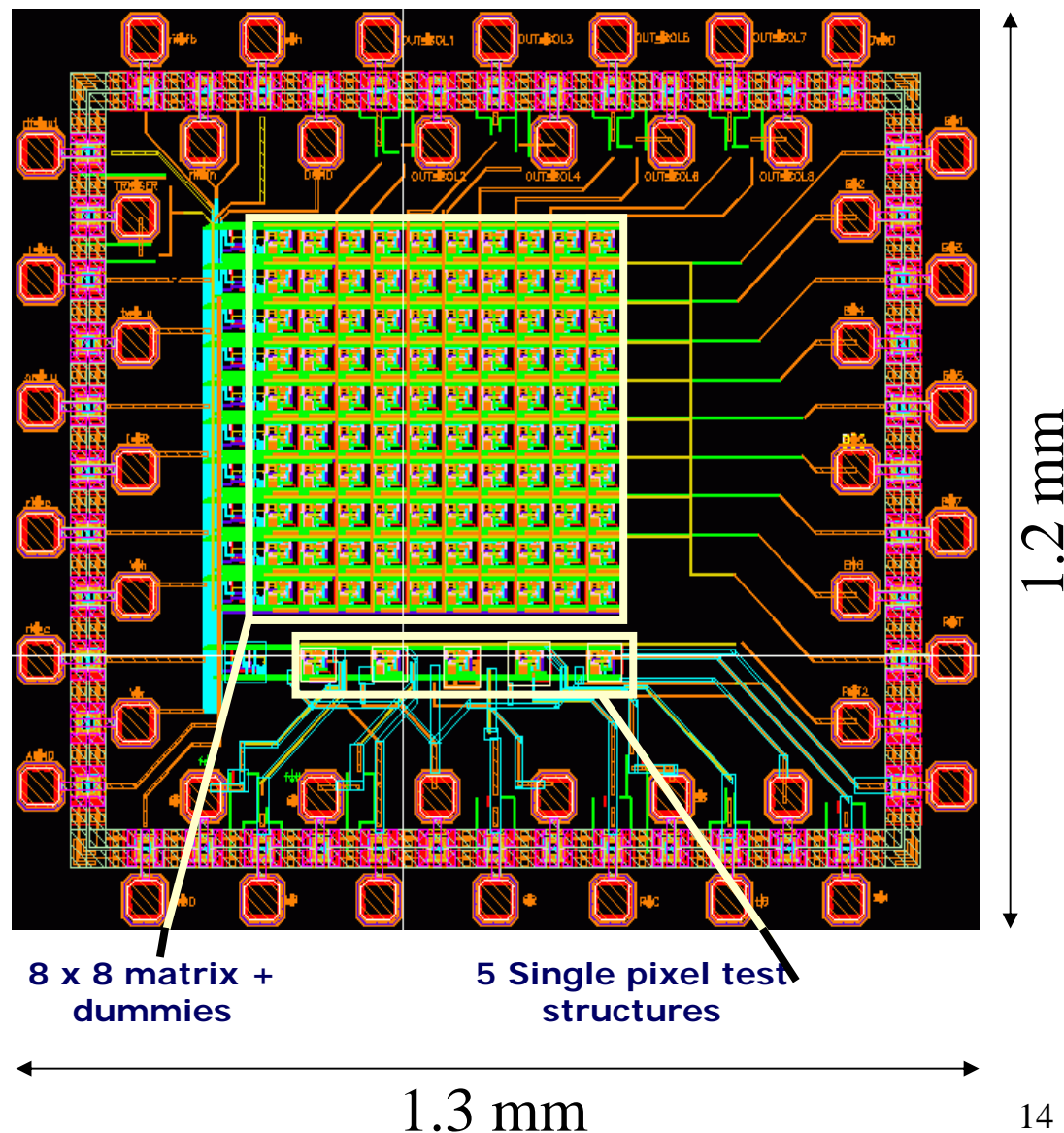
Peak value of the shaper output:

- blue - with  $\beta$  source
- green - no source



# The apsel1 chip

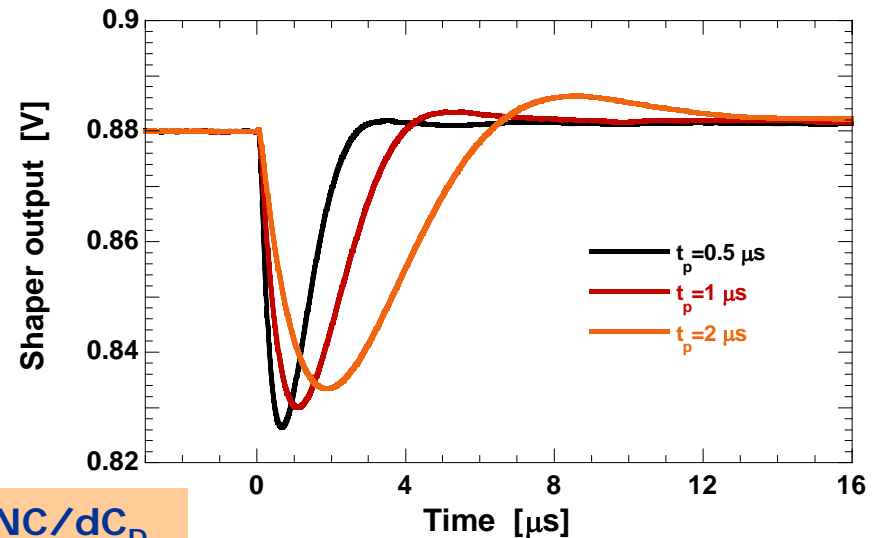
- Submitted August 2005  
(delivered Jan. 2006)
- Front end modified to address the gain and noise issues (apsel0)
- The chip includes:
  - 5 single pixel cells (with  $C_{inj}$ )
    - 1 standalone readout channel (ROC)
    - 4 Deep N-Well MAPS with different sensor area
  - an 8x8 MAPS matrix (50  $\mu\text{m}$  pitch) with a trigger signal (wired OR of the latch outputs)



# FEE Test Results

The new front-end circuit design solved the gain and noise issues raised by the 1<sup>st</sup> prototype:

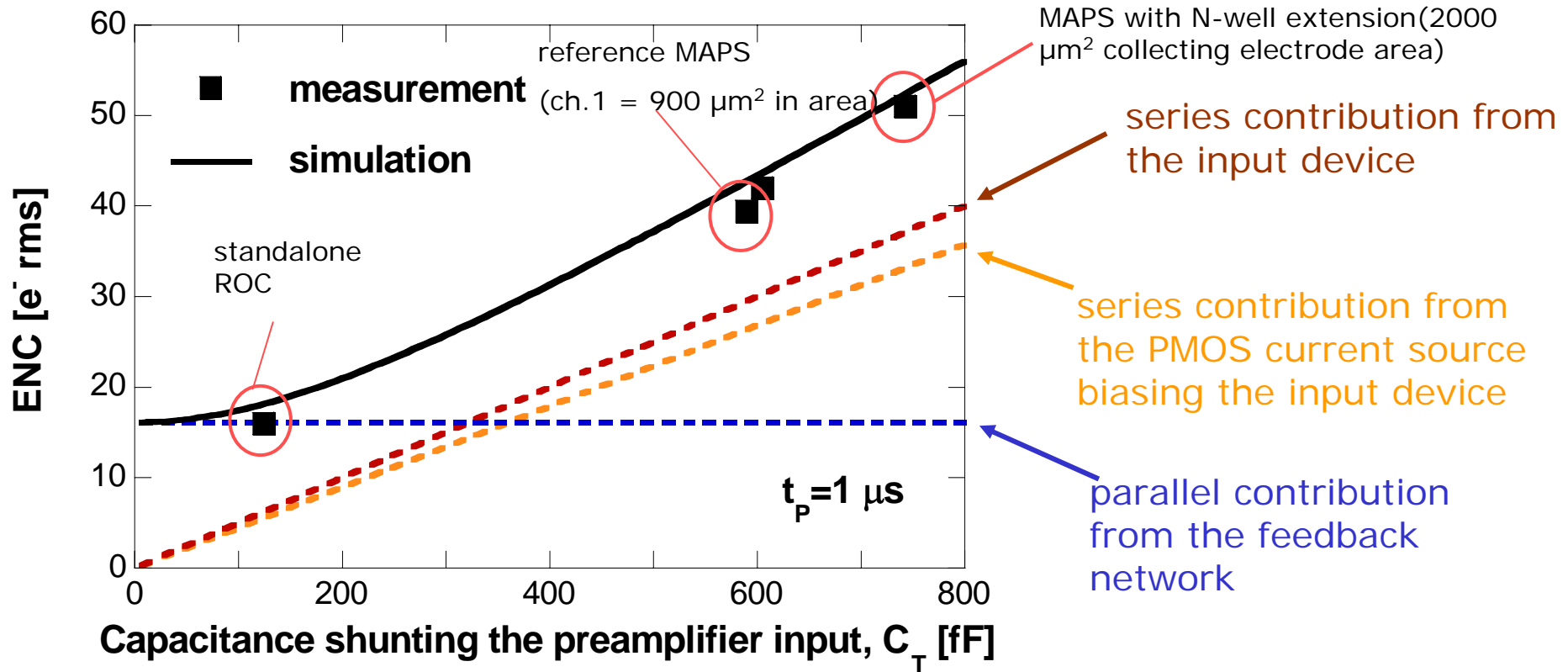
- folded cascode and active load stage implemented in the charge preamplifier
- input element:  $W/L=16/0.25$  (optimized for  $C_D=320$  fF)
- drain current in the input stage:  $30 \mu\text{A}$  (dissipation:  $P=60 \mu\text{W}/\text{channel}$ )



Response to a  $750 e^-$  pulse

Peaking time [ $\mu\text{s}$ ]	ENC [ $e^-$ rms]	Charge sensitivity [mV/fC]	dENC/d $C_D$ [ $e^-/\text{pf}$ ]
0.5	41	466	70
1	39	432	68
2	39	406	68

# Contributions to ENC



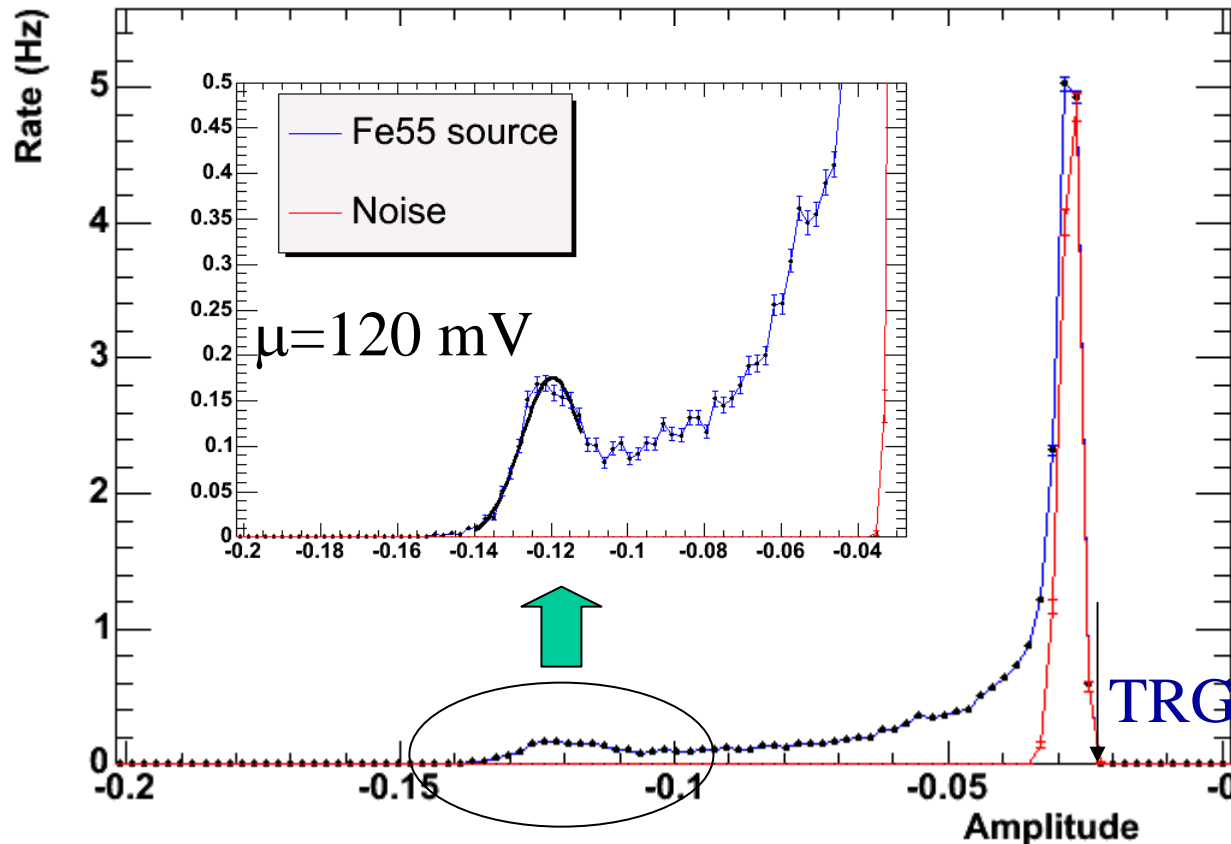
$$C_T = C_D + C_{inj} + C_{in} + C_F$$

$$C_D = 460 \text{ fF for ch.1}$$

$$C_{inj} = 60 \text{ fF}, C_{in} = 40 \text{ fF}, C_F = 8 \text{ fF}$$

# Single channel response to soft X-rays from Fe<sup>55</sup>

$$Gain_{Fe^{55}} = \frac{V_{peak} (mV)}{1640 \cdot 1.6 \cdot 10^{-4} fC} = 457 (mV / fC)$$



The events on the right of the peak are due to charge partially collected.

$$\frac{S}{N} = 30$$

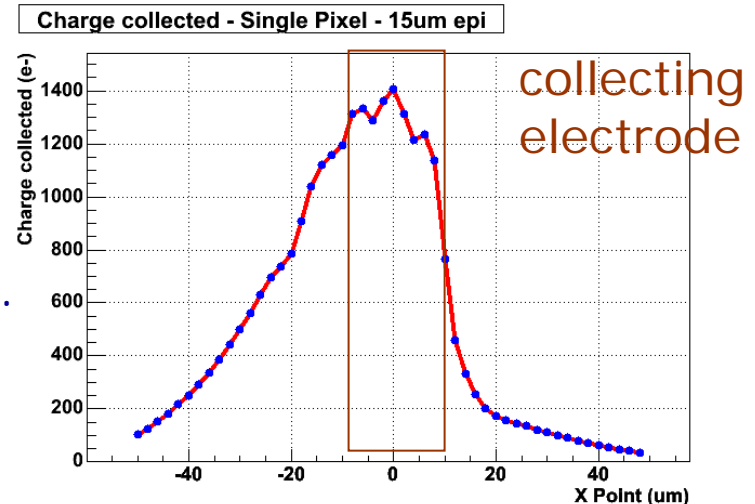
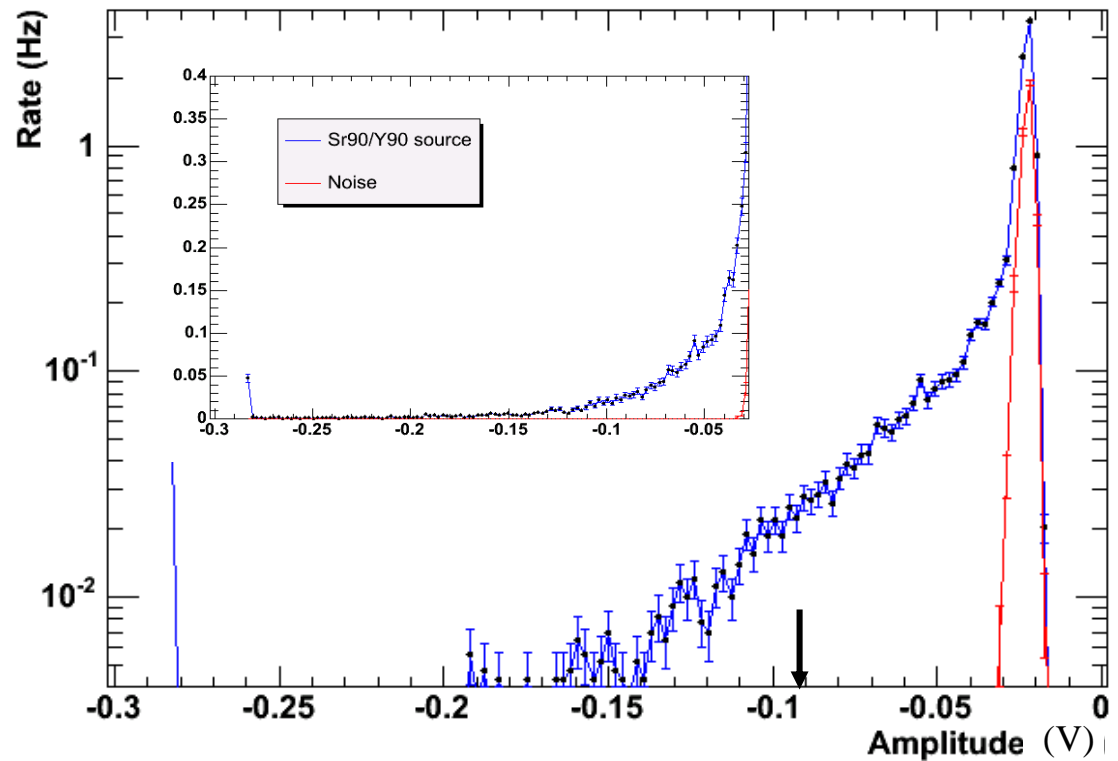
Fe<sup>55</sup> : 5.9 keV

TRG cut=20 mV  
(Volt)

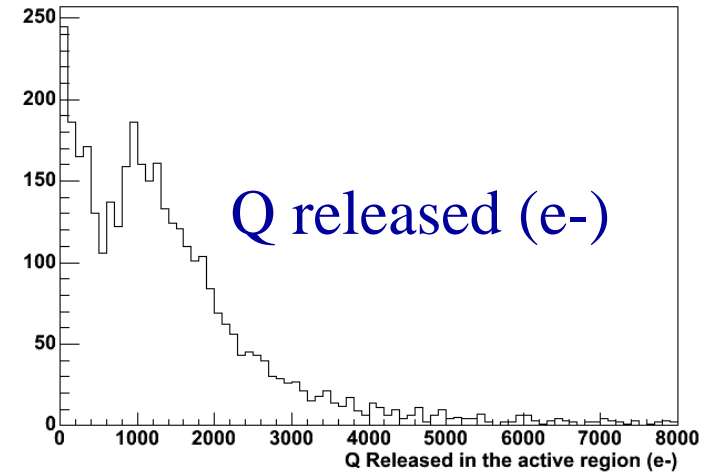
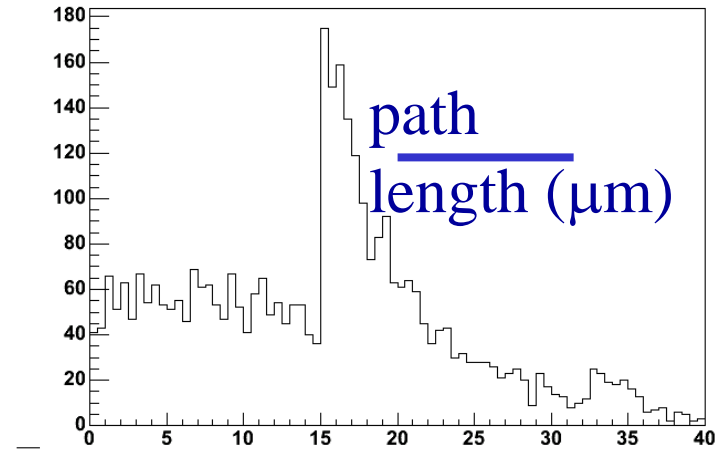
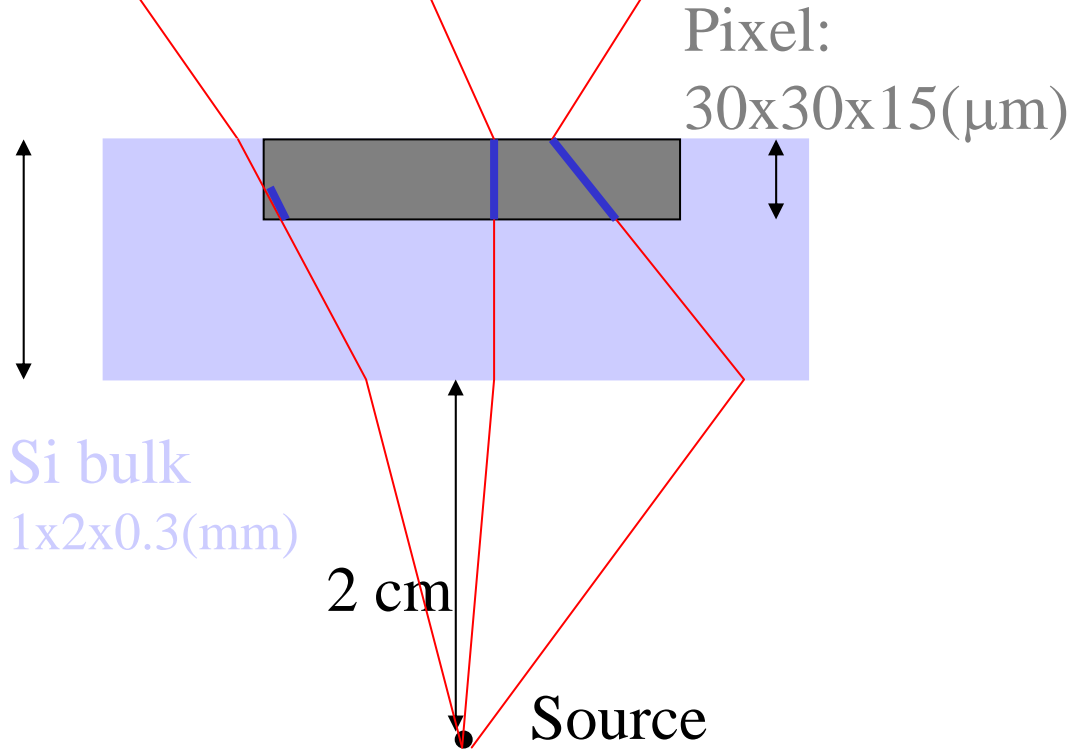
# Single channel response to $\beta$

- Observed a clear signal
- Continuous spectrum of collected Energy!
- WHY “Landau” NOT VISIBLE?
- Two effects conspires:
  - **Released Energy:** (from Geant4 simulations) the released energy strongly depends (through multiple scattering) on the amount of material supporting the die. Mechanical differences (apsel1,apsel0) in the assemblies may obscure the peak.
  - **Collected Energy:** efficiency not uniform, contribution from a broad region outside the **collecting electrode**.

Spectrum (pixel in coinc. with scint.)



# Geant simulation ( $\beta$ -rays): basic geometry

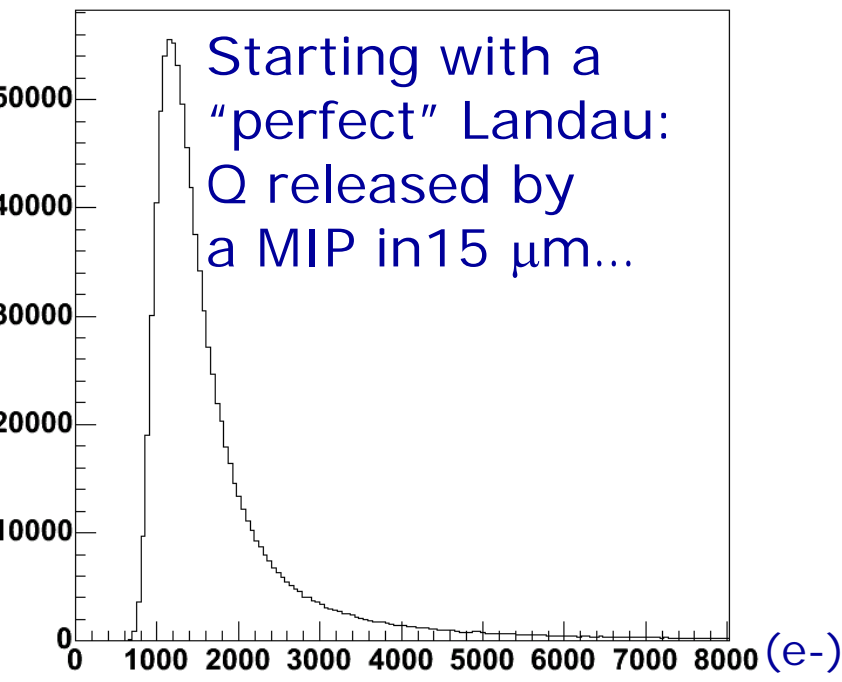


Geant4 simulations indicate that material used to support the sensor might produce large (multiple scattering) effects due to the very low momentum of the impinging electrons.

- The chip holders (apsel0 vs aysel1) are slightly different: Inserted a  $300 \mu\text{m}$  thick Al radiator (with a  $1 \text{ mm}$  hole) to dissipate power (on the back) and mount the (apsel1) die.

# The effect of the not uniform efficiency region

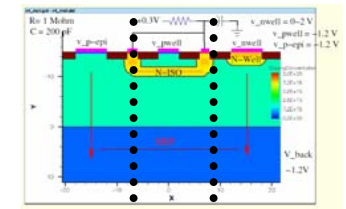
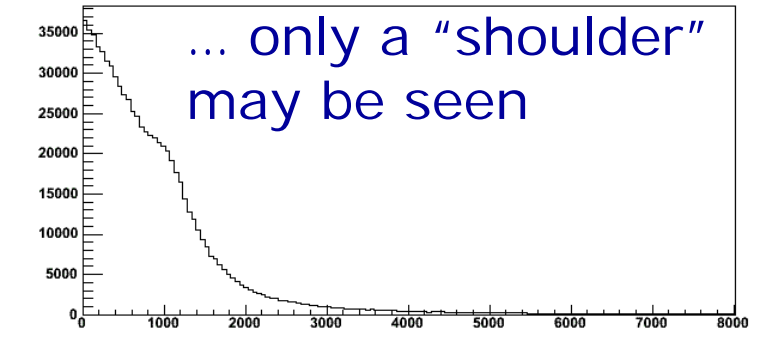
Q released



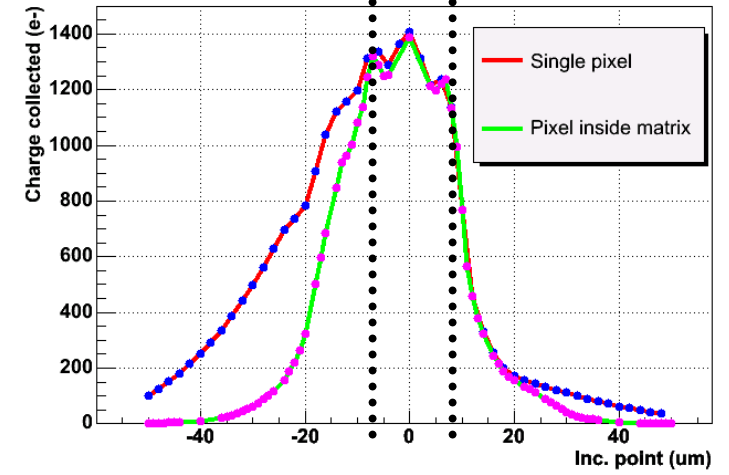
$$Q(\text{collected}, r) = Q(\text{released}, r) * \epsilon(r)$$



Q collected



Charge collection efficiency (from ISE simulation)



The larger the region, the smaller the shoulder (.. and less sensitive to a deconvolution ...)  
 This effect is expected to be less significant in the matrix.

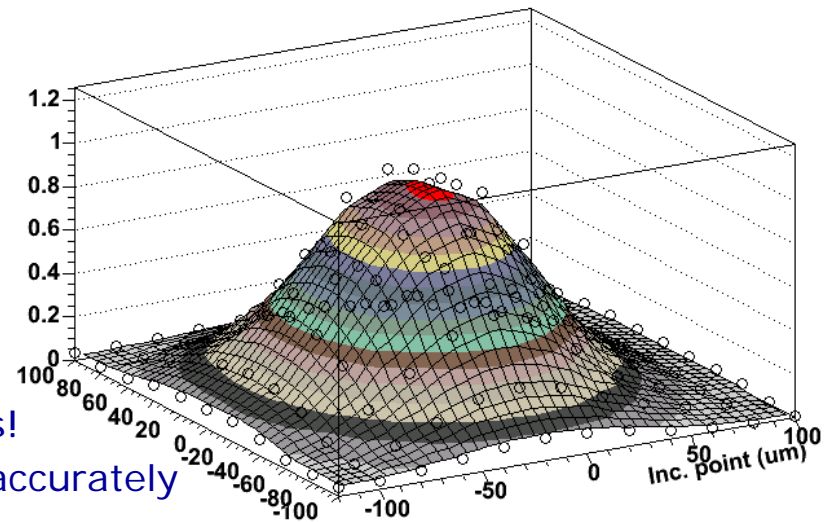
# Further investigations

- Still investigating the best set-up to enhance the “Landau” (MIP crossing  $\perp$  the sensitive region)
- The actual spectrum with  $\beta$ -rays (low energy e-) prevents us from measuring a Signal/Noise ratio for MIP for apsel1.

Relying on the measurements on Fe<sup>55</sup>, we can expect:

$$\frac{S}{N} \approx 22 \text{ for MIP}$$

CCE with laser spot on apsel1



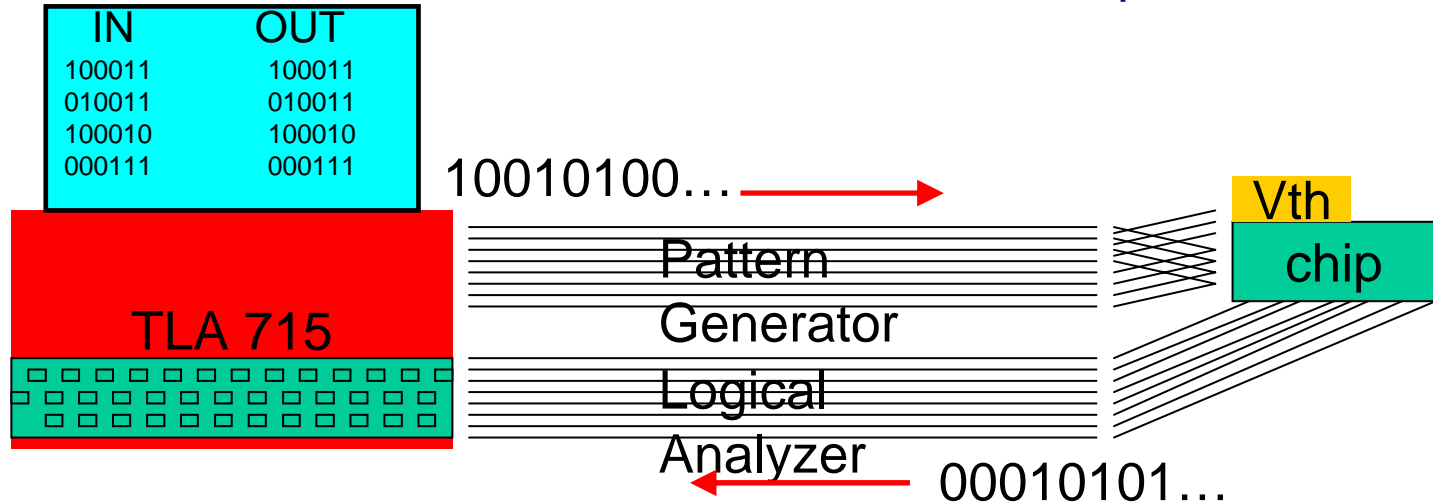
- A scan with an I.R. laser with a small spot size used to measure CCE efficiency across the pixel cell, for:

- comparison with simulations
- differences apsel0/apsel1
  - Dummy metals are causing reflections!
  - vertical position must be reproduced accurately

Work in progress

# Test of the matrix

- Available (only) the digital info (latch output)
- Unique discriminator Threshold value for all the pixels

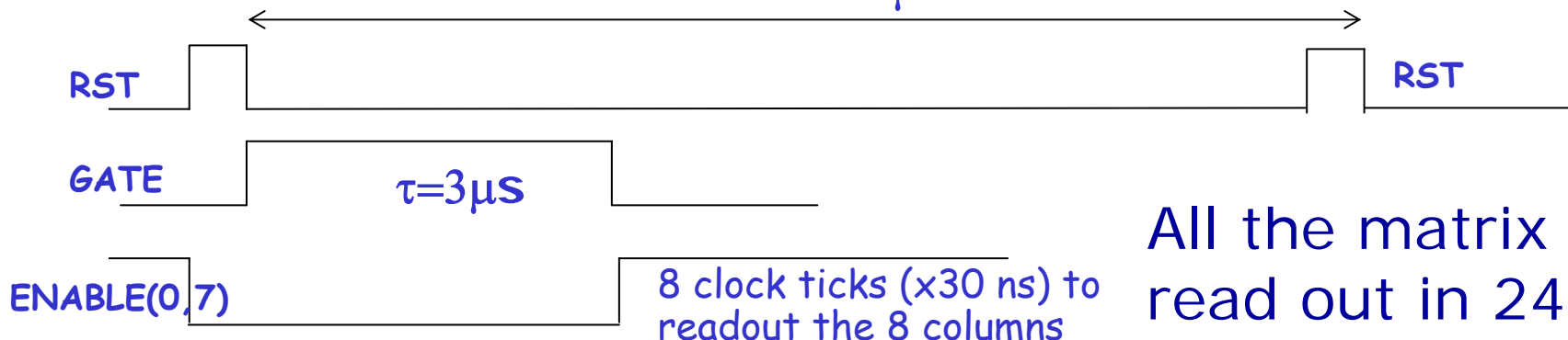


- Sequential readout of the matrix successfully tested up to 30 MHz
- Test Results:
  - Noise scan (latch firing efficiency vs discriminator thr.)
    - Significant Threshold dispersion
    - How to cure the effect
  - Threshold scan with trigger on external pulse
    - I.R. laser
    - Response to radioactive sources ( $\beta$  and X) w/o analog info:
      - ✓ Integral rate vs Thr. → differential rate = Energy spectrum

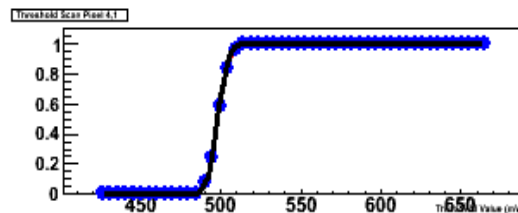
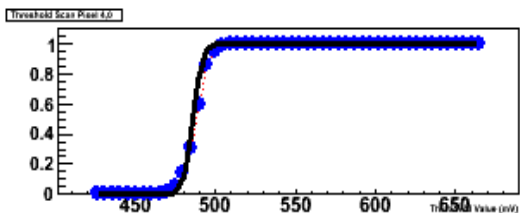
# Noise scan

$T=30\mu\text{m}$

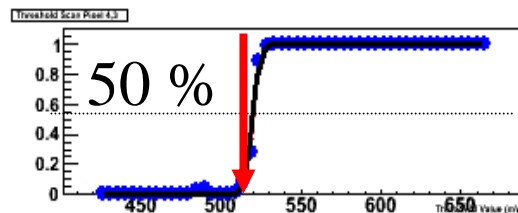
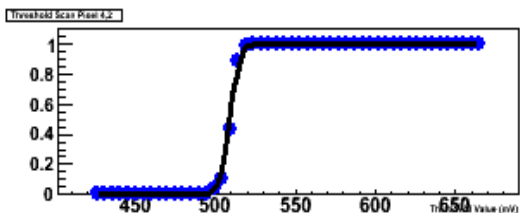
Sequence:



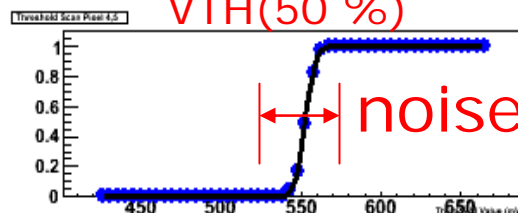
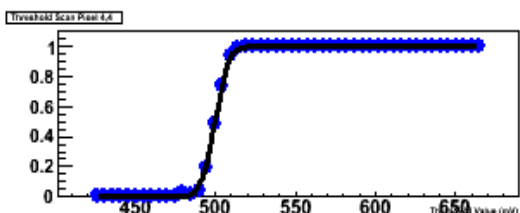
All the matrix read out in 240 ns



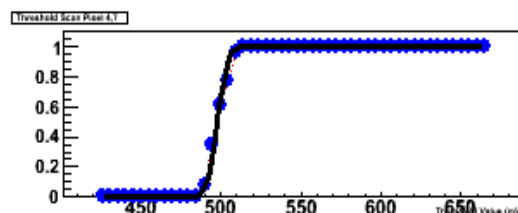
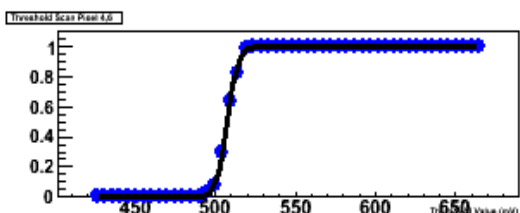
Typical "S" curves:  
Occupancy vs. Threshold (mV) with error function fit for the pixel of one row (5 mV step)



VTH(50 %) provides an estimate of the baseline **offset** of the shaper output



**offset**

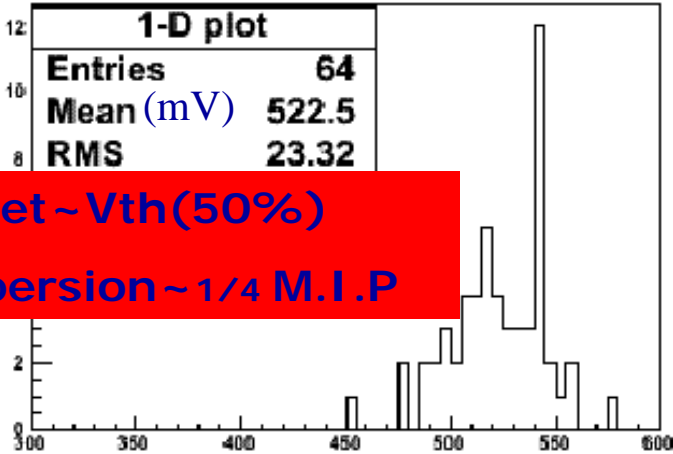


SHAPER OUT:

# Vth(50%) dispersion and noise on the matrix

In a CMOS process threshold voltage (and channel transconductance  $g_m$ ) typically affected by microscopic variations in physical quantities (e.g. oxide thickness, dopant concentration ...)

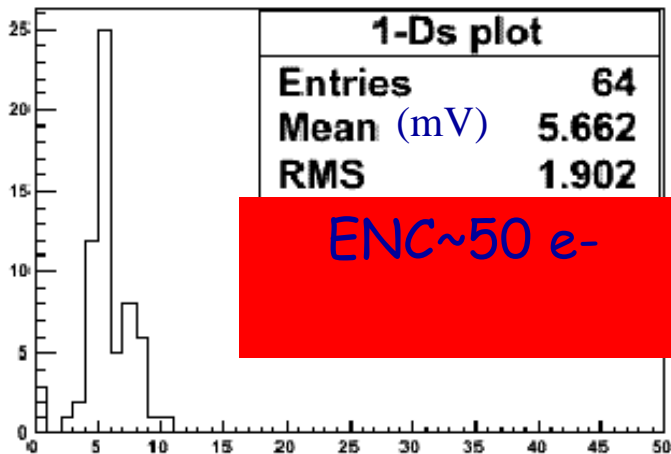
Dispersion of the fitted thr0.5



Offset ~ Vth(50%)

Dispersion ~ 1/4 M.I.P

Dispersion of the fitted noise



ENC ~ 50 e-

- Possible to act on the device dimensions:

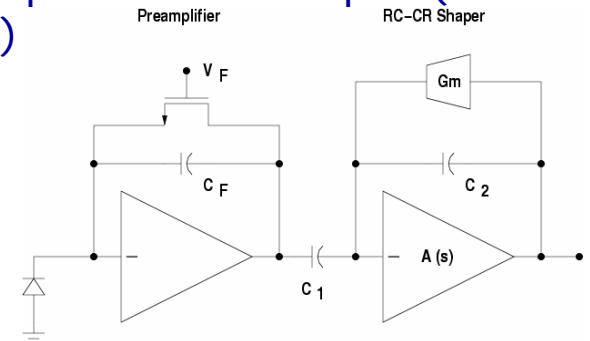
$$\sigma_{V_{th}^{MOS}} = \frac{A_{V_{th}^{MOS}}}{\sqrt{WL}}$$

$A_{V_{th}^{MOS}}$  constant provided by the foundry

- The dominant contribution to the threshold dispersion is expected to come from the dispersion on the shaper output baseline.

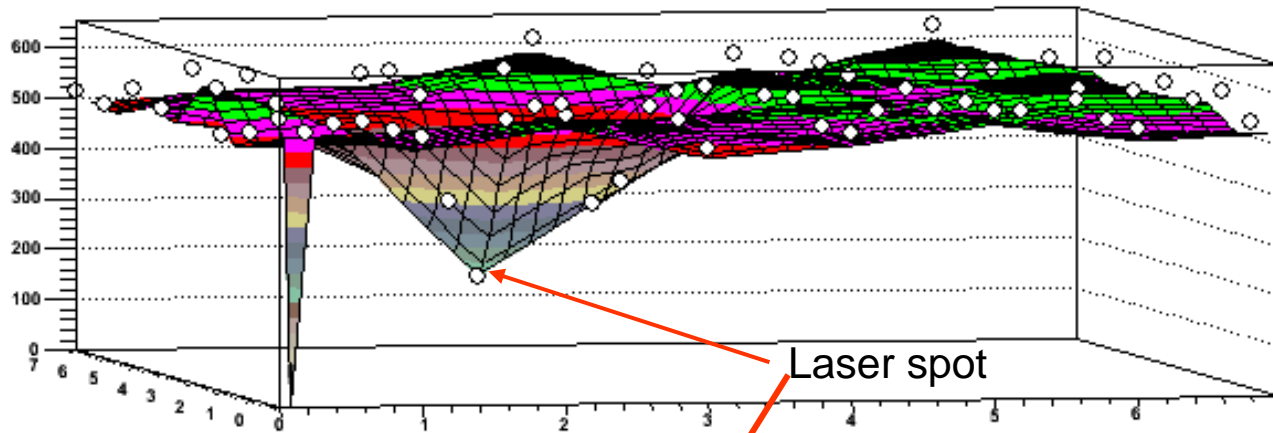
- In the Apse1 chip, MC simulations in fair agreement with the results from the characterization of the matrix.

- Significant reduction (~factor 10) of the dispersion obtained by redesigning of the transconductor and part of the shaper (without increasing the ENC)

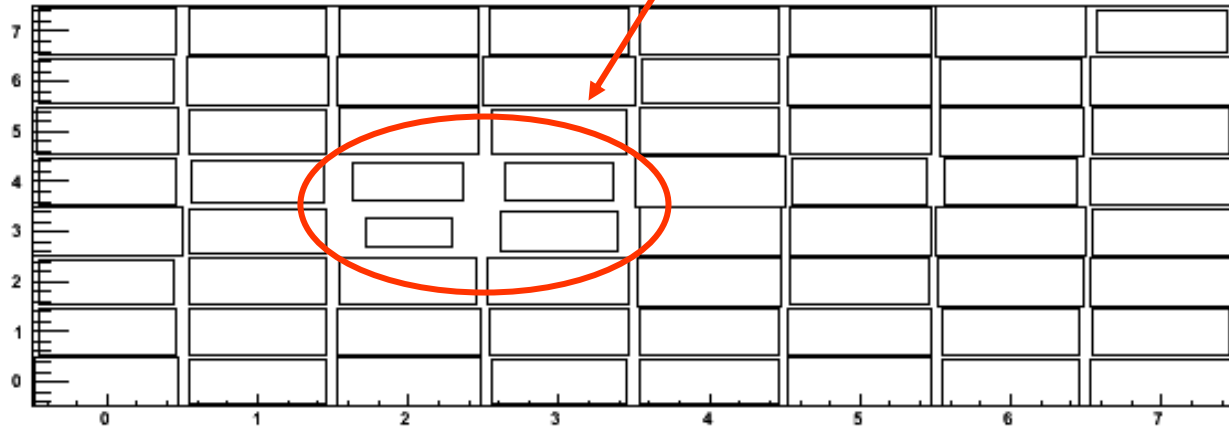


# I.R. (1060 nm) laser

Graph2D



Fitted thr offset



2-D plot	
Max(x)	64
Mean(x)	3.555
Mean(y)	3.498
RMS(x)	2.364
RMS(y)	2.317
σ	0
τ	32401
σ	0

The laser beam ( $\sigma_x = \sigma_y \sim 10 \mu\text{m}$ , Power  $\sim 150 \text{ fJ/pulse}$ ) releases  $\sim 3000 \text{ e-}$  in  $15 \mu\text{m}$  of active volume (metal dummies cause reflection).  
First indication on the cluster size for charge uniformly distributed.

## TH-scan with X-ray and $\beta$ sources

During these measurements we have observed various effects that distort the resulting energy spectra not-trivially, hence we choose not to show the spectra at this time.

We are investigating the origin of these effects (cross-talk among the pixels in the matrix, ground bounce, ...?) both by checking at the layout level and with specific diagnostic tests.

# Toward Apse12

We are working on the design of the next chip:

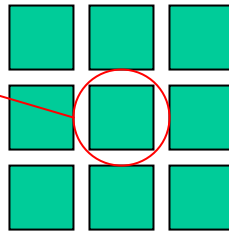
- Matrix 8x8 (same read out):
  - FE modified to reduce the Thr. Dispersion
  - Insert analog info on a selection of pixels
  - Inj. Capacitance for ext. stimulus
  - Hopefully we can cure the “cross-talk”

} for diagnostic  
purpose

- Single pixel channels with different collecting electrode

Area → micromatrix 3x3 with analog/digital info available

for the central pixel



- A lot of work ongoing toward sparsification implemented at the pixel level (verilog simulation phase): test structures to test digital blocks of readout architecture will be implemented.

# Conclusions (I)

- A novel kind of CMOS MAPS (deep N-well MAPS) has been designed and fabricated in a 130 nm CMOS technology:
  - A deep n-well used as the sensitive electrode
  - The standard readout channel for capacitive detectors used to amplify the charge signal and extract digital information
- The first prototype, `apsel0`, was tested and demonstrated that the sensor has the capability of detecting ionizing radiation.
- In the new chip, `apsel1`, noise and gain issues (present in `apsel0`) have been correctly addressed.
- Single pixel measurements confirm the observation of soft X and  $\beta$  rays
- The 8x8 (simple) matrix has been successfully readout

# Conclusions (II)

- Still ongoing analysis of the response to radioactive sources from the pixel matrix
- Next submission (Aug. 06) focused on:
  - Cure the threshold dispersion
  - More diagnostic features on pixel matrix
  - Test digital blocks toward data sparsification
- Our final goal: to develop a matrix with sparsified readout suitable to be used in a trigger (L1) system based on associative memories.

# The SLIM5 collaboration (Silicon with Low Interaction with Material – CSN5 INFN)

S. Bettarini<sup>1,2</sup>, A. Bardi<sup>1,2</sup>, G. Batignani<sup>1,2</sup>, F. Bosi<sup>1,2</sup>, G. Calderini<sup>1,2</sup>, R. Cenci<sup>1,2</sup>, M. Dell'Orso<sup>1,2</sup>, F. Forti<sup>1,2</sup>, P. Giannetti<sup>1,2</sup>, M. A. Giorgi<sup>1,2</sup>, A. Lusiani<sup>2,3</sup>, G. Marchiori<sup>1,2</sup>, F. Morsani<sup>2</sup>, N. Neri<sup>2</sup>, E. Paoloni<sup>1,2</sup>, G. Rizzo<sup>1,2</sup>, J. Walsh<sup>2</sup>,

C. Andreoli<sup>4,5</sup>, E. Pozzati<sup>4,5</sup>, L. Ratti<sup>4,5</sup>, V. Speziali<sup>4,5</sup>,

M. Manghisoni<sup>5,6</sup>, V. Re<sup>5,6</sup>, G. Traversi<sup>5,6</sup>,

L. Bosisio<sup>7</sup>, G. Giacomini<sup>7</sup>, L. Lanceri<sup>7</sup>, I. Rachevskaia<sup>7</sup>, L. Vitale<sup>7</sup>,

M. Bruschi<sup>8</sup>, B. Giacobbe<sup>8</sup>, N. Semprini<sup>8</sup>, R. Spighi<sup>8</sup>, M. Villa<sup>8</sup>, A. Zoccoli<sup>8</sup>,

D. Gamba<sup>9</sup>, G. Girauda<sup>9</sup>, P. Mereu<sup>9</sup>,

G.F. Dalla Betta<sup>10</sup>, G. Soncini<sup>10</sup>, G. Fontana<sup>10</sup>, L. Pancheri<sup>10</sup>,

G. Verzellesi<sup>11</sup>

<sup>1</sup>Università degli Studi di Pisa, <sup>2</sup>INFN Pisa,

<sup>3</sup>Scuola Normale Superiore di Pisa,

<sup>4</sup>Università degli Studi di Pavia, <sup>5</sup>INFN Pavia,

<sup>6</sup>Università degli Studi di Bergamo,

<sup>7</sup>INFN Trieste and Università degli Studi di Trieste

<sup>8</sup>INFN Bologna and Università degli Studi di Bologna

<sup>9</sup>INFN Torino and Università degli Studi di Torino

<sup>10</sup>Università degli Studi di Trento and INFN Padova

<sup>11</sup>Università degli Studi di Modena e Reggio Emilia and INFN Padova

## 4 Workpackages:

**.1 MAPS and Front End Electronics**

**.2 Detectors on high-resistivity Silicon**

**.3 Trigger / DAQ**

**.4 Mechanics/Integration/Test-Beam**